Remote Sensing of Environment xxx (2016) xxx–xxx

Contents lists available at ScienceDirect

Remote Sensing of Environment

journal homepage: www.elsevier.com/locate/rse

Assessing the role of climate and resource management on groundwater dependent ecosystem changes in arid environments with the Landsat archive

Justin Huntington [a,b,*,1], Kenneth McGwire [a], Charles Morton [a], Keirith Snyder [c], Sarah Peterson [d], Tyler Erickson [e], Richard Niswonger [f], Rosemary Carroll [a], Guy Smith [a], Richard Allen [g]

[a] Desert Research Institute, Reno, Nevada, United States
[b] Western Regional Climate Center, Reno, Nevada, United States
[c] USDA Agricultural Research Service, Reno, Nevada, United States
[d] Bureau of Land Management, Reno, Nevada, United States
[e] Google, Inc., Mountain View, California, United States
[f] U.S. Geological Survey, Menlo Park, California, United States
[g] University of Idaho, Kimberly, Idaho, United States

ARTICLE INFO

Article history:
Received 29 August 2015
Received in revised form 31 May 2016
Accepted 5 July 2016
Available online xxxx

Keywords:
Landsat
NDVI
Cross-sensor calibration
Groundwater dependent ecosystems
Riparian restoration
Groundwater pumping
Phreatophytes
Complementary relationship
Evaporative demand

ABSTRACT

Groundwater dependent ecosystems (GDEs) rely on near-surface groundwater. These systems are receiving more attention with rising air temperature, prolonged drought, and where groundwater pumping captures natural groundwater discharge for anthropogenic use. Phreatophyte shrublands, meadows, and riparian areas are GDEs that provide critical habitat for many sensitive species, especially in arid and semi-arid environments. While GDEs are vital for ecosystem services and function, their long-term (i.e. ~30 years) spatial and temporal variability is poorly understood with respect to local and regional scale climate, groundwater, and rangeland management. In this work, we compute time series of NDVI derived from sensors of the Landsat TM, ETM+, and OLI lineage for assessing GDEs in a variety of land and water management contexts. Changes in vegetation vigor based on climate, groundwater availability, and land management in arid landscapes are detectable with Landsat. However, the effective quantification of these ecosystem changes can be undermined if changes in spectral bandwidths between different Landsat sensors introduce biases in derived vegetation indices, and if climate, and land and water management histories are not well understood. The objective of this work is to 1) use the Landsat 8 under-fly dataset to quantify differences in spectral reflectance and NDVI between Landsat 7 ETM+ and Landsat 8 OLI for a range of vegetation communities in arid and semiarid regions of the southwestern United States, and 2) demonstrate the value of 30-year historical vegetation index and climate datasets for assessing GDEs. Specific study areas were chosen to represent a range of GDEs and environmental conditions important for three scenarios: baseline monitoring of vegetation and climate, riparian restoration, and groundwater level changes. Google's Earth Engine cloud computing and environmental monitoring platform is used to rapidly access and analyze the Landsat archive along with downscaled North American Land Data Assimilation System gridded meteorological data, which are used for both atmospheric correction and correlation analysis. Results from the cross-sensor comparison indicate a benefit from the application of a consistent atmospheric correction method, and that NDVI derived from Landsat 7 and 8 are very similar within the study area. Results from continuous Landsat time series analysis clearly illustrate that there are strong correlations between changes in vegetation vigor, precipitation, evaporative demand, depth to groundwater, and riparian restoration. Trends in summer NDVI associated with riparian restoration and groundwater level changes were found to be statistically significant, and interannual summer NDVI was found to be moderately correlated to interannual water-year precipitation for baseline study sites. Results clearly highlight the complementary relationship between water-year PPT, NDVI, and evaporative demand, and are consistent with regional vegetation index and complementary relationship studies. This work is supporting land and water managers for evaluation of GDEs with respect to climate, groundwater, and resource management.

* Corresponding author at: Western Regional Climate Center, Reno, Nevada, United States
E-mail address: justin.huntington@dri.edu (J. Huntington).
[1] 2215 Raggio Parkway, Reno, Nevada, 89512.

http://dx.doi.org/10.1016/j.rse.2016.07.004
0034-4257/

1. Introduction

Groundwater dependent ecosystems (GDEs) rely on near-surface groundwater. They provide critical habitat for many sensitive species in arid and semi-arid environments and include phreatophyte shrub lands, meadows, spring areas, and riparian zones. Improved understanding of how climate and anthropogenic impacts affect the spatiotemporal variability of GDEs is needed to increase the effectiveness of ecosystem assessments, monitoring, adaptive management frameworks, and designations of protected areas (e.g. sage-grouse habitat). However, the lack of observations provides a constraint on the utilization of data for decision-making and scientific research. Long-term remote sensing observations from the Landsat archive have repeatedly demonstrated value for ecosystem monitoring, and are increasingly being used to evaluate GDE changes relative to changing climate, drought, groundwater pumping, and agricultural disturbance (Elmore et al., 2003; Groeneveld, 2008; Yang et al., 2011; Pritchett and Manning, 2012; Nguyen et al., 2014; Homer et al., 2015). The longevity and continuity of measurements from sensors in the lineage of Landsat's Thematic Mapper (TM), Enhanced Thematic Mapper Plus (ETM+), and Operational Land Imager (OLI), provide important baseline and current conditions that would not otherwise be attainable.

With free access to the Landsat archive, resource managers can now rely on long time series of Landsat derived vegetation index information in order to evaluate important factors affecting vegetation vigor within GDEs, including natural background variability due to climate, weather, land surface-atmospheric feedbacks, and anthropogenic factors such as land use, restoration, and groundwater pumping. However, long time series analysis with Landsat must deal with number of challenges, including data storage, computational efficiency, and changes in sensor bandwidths over time (i.e. TM, ETM+, OLI). The first two issues can be easily managed with parallelized cloud computing within Google's Earth Engine (EE), a powerful new cloud computing and environmental monitoring platform. The third issue of changing sensor bandwidths and accurate interpretation of Landsat vegetation index time series, requires quantification of how changing spectral response functions between sensors interact with the spectral variability of dynamic vegetation communities (Li et al., 2013). Effective quantification of GDE changes, and the credibility of derived resource management decisions, in part, depends on the compatibility of vegetation indices derived from different sensors, and the ability to isolate the effects of climatic and natural hydrologic variability on vegetation vigor from anthropogenic effects of land and water management.

2. Objective

The objective of this work is to 1) use the Landsat 8 under-fly dataset to quantify differences in spectral reflectance and vegetation indices between Landsat 7 ETM+ and Landsat 8 OLI for a range of vegetation communities in arid and semiarid regions of the southwestern United States, and 2) demonstrate the value of 30-year historical vegetation index datasets derived from sensors of the Landsat TM, ETM+, and OLI lineage for assessing GDEs in a variety of land and water management contexts. The study approach relies on sensor cross-calibration, cloud computing of Landsat and meteorological data, and statistical evaluation of vegetation index time series relative to annual precipitation and evaporative demand, restoration, and changing groundwater levels. Landsat 7 and 8 images from a brief under-fly test period are used to develop correction factors that account for differences between ETM+ and OLI, and to assess how discrepancies may be correlated with the typical spectral reflectance curves of dominant vegetation communities within the Great Basin, USA. Two forms of atmospheric correction are used to evaluate inter-sensor variability of spectral indices: 1) the at-surface reflectance products of Landsat climate data records available through the USGS Earth Resources Observation and Science (EROS) Center Science Processing Architecture (ESPA; USGS, 2015a), and 2) the Tasumi et al. (2008) atmospheric correction algorithm that utilizes meteorological datasets within EE. Time series of corrected Normalized Difference Vegetation Index (NDVI) are analyzed for six GDE study areas within the Great Basin to demonstrate the utility of the Landsat archive for local-scale GDE assessments.

3. Study areas and background

Specific study areas were chosen to represent a range of GDEs and environmental conditions important for three scenarios: baseline monitoring of vegetation and climate, riparian restoration, and groundwater level changes (Fig. 1 and Table 1).

3.1. Baseline assessment of vegetation and climate

Spring Valley (Fig. 2a) is located in eastern Nevada, and is of interest to federal, state, and local water resource and land managers due to the potential for groundwater development. State of Nevada groundwater permit terms, along with stipulated agreements by local and federal agencies, require detailed hydrologic and biological monitoring associated with groundwater development (NSEO, 2012; Burns and Drici, 2011; BWG, 2009). The alkali shrub phreatophyte area analyzed in this study is located in the southern portion of Spring Valley, and is a primary groundwater discharge area down gradient from proposed pumping wells. Depth to groundwater within the study area ranges from 2 to 10 m below land surface (Moreo et al., 2007). Phreatophyte shrubs obtain their water requirement from surface water, groundwater, or both, through root systems that range from shallow to 15 m depth (Robinson, 1958; Glancy and Rush, 1968; Dawson and Pate, 1996). While phreatophytes within the study area consume groundwater, they primarily rely on shallow soil water derived from precipitation, and typically only consume harder to access groundwater during summer and early fall when shallow soil moisture levels are low (Dawson and Pate, 1996; Chimner and Cooper, 2004), thereby making summer phreatophyte vegetation vigor (i.e. NDVI) a function of interannual precipitation, soil moisture, and shallow groundwater level variations.

Indian Valley (Fig. 2b) is located in central Nevada and is of interest to many wildlife and land managers due to the presence of the greater sage-grouse (*Centrocercus urophasianus*), a threatened species that has been petitioned for formal protection under the Endangered Species Act (DOI, 2015). Indian Valley has been identified as priority habitat due to its high sage-grouse lek (the male's mating arena) count, remote location, and relatively undisturbed phreatophyte meadow and shrub areas (BLM, 2012). An active area of cross-disciplinary research on sage-grouse is focused on the use of climate and Landsat archives to better understanding how climate, vegetation vigor, and sage-grouse habitat co-vary in time and space, and to identify which areas are resistant to prolonged drought (Aldridge and Boyce, 2007; Homer et al., 2015; Donnelly et al., 2016).

3.2. Riparian restoration

Maggie Creek (Fig. 3a) and Susie Creek (Fig. 3b), both located in north-central Nevada, are tributaries to the Humboldt River that support Lahontan cutthroat trout (*Oncoryhnchus clarki henshawi*). This species has been federally listed under the Endangered Species Act due to its sensitivity to changes in land and water use, prolonged drought, and changing climate (Williams et al., 2015). Vegetation communities within riparian zones of Maggie and Susie Creeks are typical of the Great Basin and include both obligate and facultative herbaceous and woody phreatophyte species. The Bureau of Land Management (BLM) collaborated with federal and local government agencies, non-profit organizations, and local mining and livestock companies to implement comprehensive watershed and riparian restoration efforts beginning in the early 1990s. Restoration efforts included

Please cite this article as: Huntington, J., et al., Assessing the role of climate and resource management on groundwater dependent ecosystem changes in arid environments with the Lan..., Remote Sensing of Environment (2016), http://dx.doi.org/10.1016/j.rse.2016.07.004

Fig. 1. Study areas within the Great Basin and location of the contemporaneous Landsat 7/8 image data. The Landsat 8 under-fly dataset was acquired on WRS-2 path 38 from rows 31–38, which spans the Great Salt Lake to Mexico. The brown path represents Landsat 7 with SLC off, and the green path represents Landsat 8.

fencing, culvert replacement, prescriptive livestock grazing, and development of livestock water sources away from stream areas (Elliott et al., 2004). These efforts led to a recolonization of beaver and advanced restoration through increased shallow groundwater, stream bank storage, and habitat resilience (Williams et al., 2015).

3.3. Groundwater level changes

In the Great Basin, insufficient surface water storage requires growers to irrigate with groundwater. Groundwater pumping for irrigation often times results in lowering of the groundwater table (i.e. phreatic surface), leading to reduced phreatophyte evapotranspiration (ET) and vegetation vigor (Bredehoeft et al., 1982; Bredehoeft, 2002; Nichols, 2000, Elmore et al., 2003; Elmore et al., 2006; Naumburg et al., 2005; Cooper et al., 2006; Patten et al., 2008; Groeneveld, 2008). Shallow groundwater and spring areas within Fish Lake Valley, Nevada (Fig. 4a) and Snake Valley, Utah, (Fig. 4b) respectively, were chosen to illustrate multi-year declines of shallow groundwater levels and vegetation vigor associated with groundwater pumping. These areas support obligate and facultative herbaceous and woody phreatophyte species, and associated fauna. The spring study area in Snake Valley, Needle Point Spring, is the subject of litigation between federal agencies and local irrigators

Table 1
Study area names, locations, Landsat path and row, and vegetation and groundwater information.

Study area	Location (lat, long)	Altitude (m)	WRS-2 path/row	Vegetation class	Water table (m below land surface)	Plant types
Spring Valley, NV	38.8010, −114.4760	1758	39/33	Alkali shrub	2–10	Greasewood, sagebrush, saltgrass
Indian Valley, NV	38.8010, −117.5000	2247	41/33	Meadow	0.5–2.5	Greasewood, sagebrush, saltgrass, meadow grass
Maggie Creek, NV	40.8860, −116.1870	1599	41/32	Riparian	0–2	Willow, sedge, rush
Susie Creek, NV	40.8350, −116.0242	1564	41/32	Riparian	0–2	Willow, sedge, rush
Fish Lake Valley, CA/NV	37.8036,-118.0667	1476	41/34	Alkali shrub	4–10	Greasewood, saltgrass
Snake Valley, UT/NV	38.7556, −114.0296	1662	39/33	Wetland	0–3	Cattail, greasewood, sagebrush, saltgrass

Please cite this article as: Huntington, J., et al., Assessing the role of climate and resource management on groundwater dependent ecosystem changes in arid environments with the Lan..., Remote Sensing of Environment (2016), http://dx.doi.org/10.1016/j.rse.2016.07.004

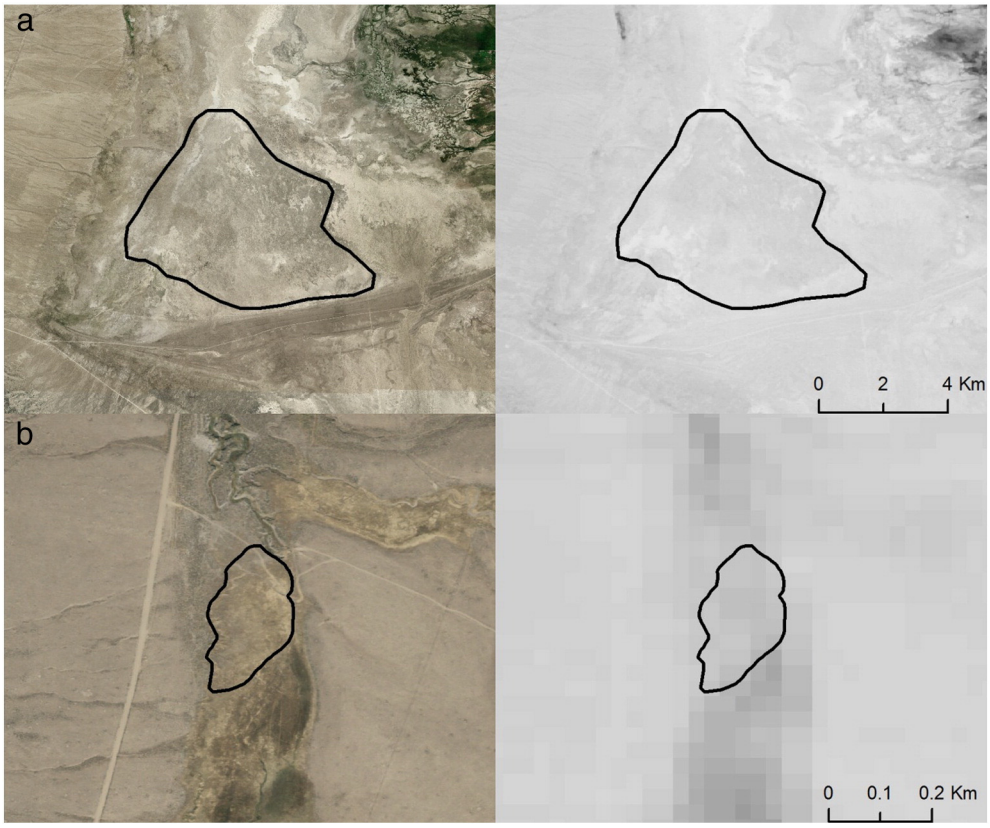

Fig. 2. Spring Valley alkali shrub (a) and Indian Valley meadow (b) natural variability study areas (black polygons). 2006 National Airborne Imagery Program (NAIP) imagery (left) and April–October 2014 Landsat 8 median NDVI (right). NDVI values linearly scaled and range from 0.0 (white) to 0.8 (black).

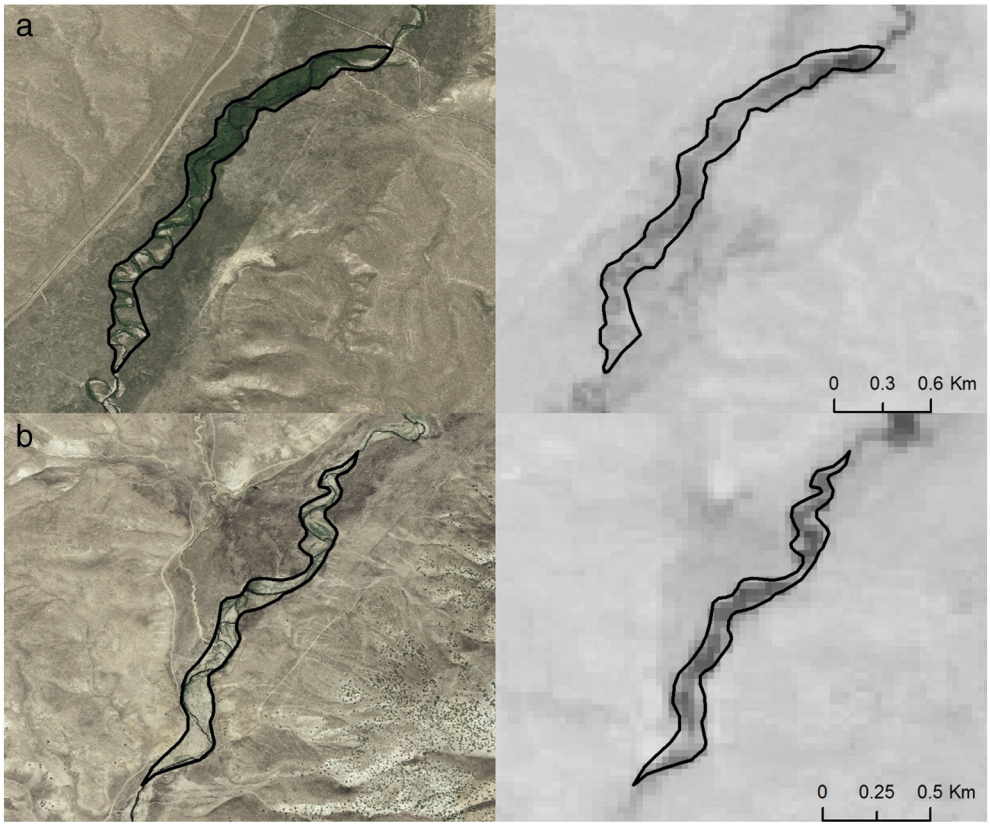

Fig. 3. Maggie Creek (a) and Susie Creek (b) riparian zone study areas (black polygons). 2006 NAIP imagery (left) and April–October 2014 Landsat 8 median NDVI (right). NDVI values linearly scaled and range from 0.0 (white) to 0.8 (black).

Please cite this article as: Huntington, J., et al., Assessing the role of climate and resource management on groundwater dependent ecosystem changes in arid environments with the Lan..., Remote Sensing of Environment (2016), http://dx.doi.org/10.1016/j.rse.2016.07.004

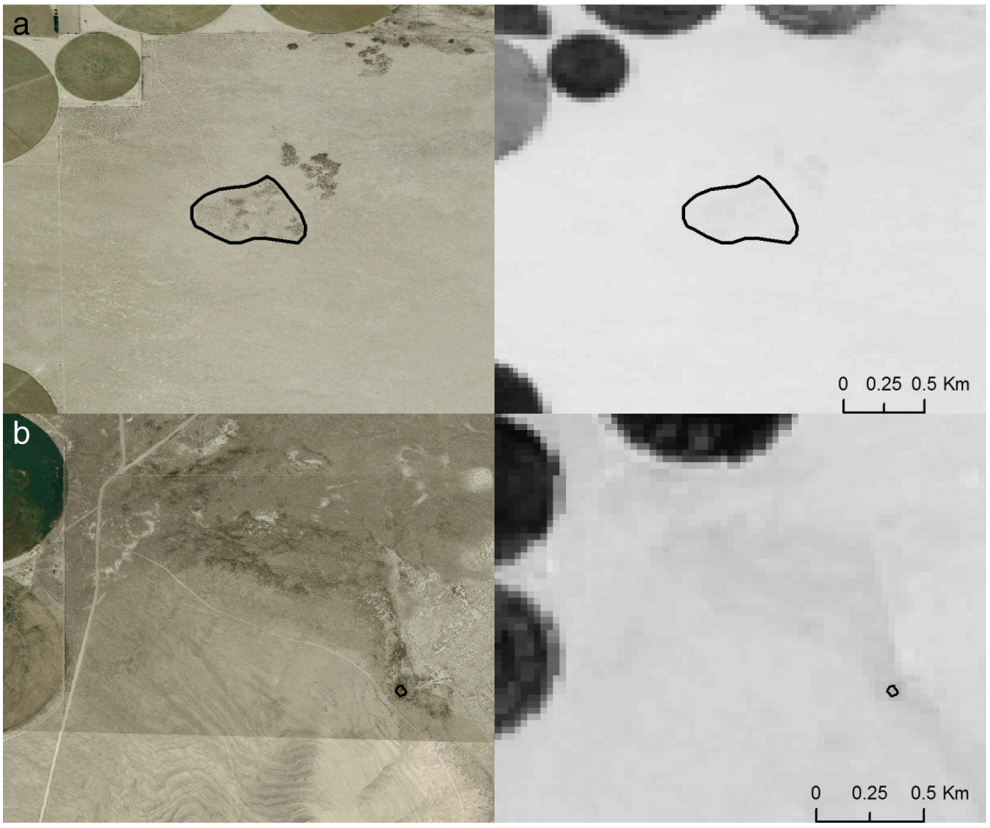

Fig. 4. Fish Lake Valley shallow groundwater (a) and Snake Valley Needle Point spring (b) groundwater change study areas (black polygons). 2006 NAIP imagery (left) and April–October 2014 Landsat 8 median NDVI (right). NDVI values linearly scaled and range from 0.0 (white) to 0.8 (black).

since the spring ceased to flow in 2001 (Halford, 2015; Childress and Smith, 2015).

4. Methods

Landsat data processing for each study area was performed through the development of Python computer programs that use the EE application programming interface (API) to access Landsat and hourly meteorological data archives. The processing workflow implements simple automated cloud masking (Irish et al., 2006), integration of hourly meteorological data for atmospheric correction and at-surface reflectance estimation (Tasumi et al., 2008), and computation of NDVI from 1985 to the present. Programming within the EE API allowed efficient scene selection and processing of 403 Landsat images collected over the six study sites (average of 67 images per study site from 1985 to 2014).

4.1. Sensor cross-calibration

The bandwidths of spectral channels on Landsat satellites have changed over time. Fig. 5 illustrates the spectral response functions of red (TM: 630–690 nm, ETM+: 630–690 nm, OLI: 640–670 nm) and near infrared (NIR; TM: 760–900 nm, ETM+: 770–900 nm, OLI: 850–880 nm) bands of Landsats 5, 7, and 8 along with representative spectra from Clark et al. (2007) of five plant species that are found in the study area (fir, juniper, piñon, sagebrush, and rabbitbrush). ETM+ response functions are seen to be relatively similar to the original TM, while the bandwidths of the OLI sensor are narrowed, particularly for the NIR band. Steven et al. (2003) suggest that there is a 2% increase in NDVI from TM to ETM+, but their result appears to have been biased upwards by questionable outliers that perhaps should have been removed (Steven et al., 2003, Fig. 3). Martínez-Beltrán et al. (2009) found increases in NDVI from TM to ETM+ to be <1%, and Vogelmann et al. (2001) support the interchangeability of the two sensors, so this analysis made no attempt to compensate between TM and ETM+. However, the more dramatic difference of OLI spectral bands has been identified as requiring attention (Li et al., 2013; Roy et al., 2016).

The effect of changes in the OLI spectral bands for vegetation in the Great Basin was assessed using images from OLI and ETM+ that were acquired within 7 min of each other on March 29, 2013 during the "under-fly" testing of the Landsat 8 system (Roy et al., 2014; USGS, 2015b). This under-fly dataset was acquired on WRS-2 path 38 from rows 31–38, which spanned the Great Salt Lake to Mexico (Fig. 1). Only rows 33–37 were used in this analysis, as the others had too much cloud cover or haze to be useful. Atmospherically corrected OLI and ETM+ images were intersected with up to 54 natural vegetation

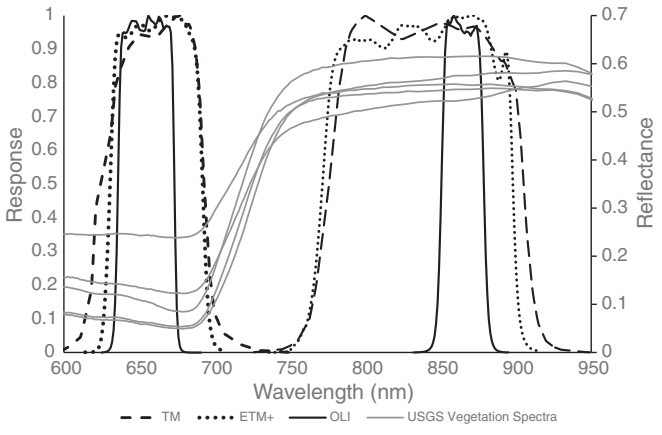

Fig. 5. Spectral response functions of red and near infrared bands for TM (630–690 nm, 760–900 nm), ETM+ (630–690 nm, 850–880 nm), and OLI along with plant type spectra (gray lines) for fir, juniper, piñon, sagebrush, and rabbit brush from a USGS spectral database (ENVI software library file usgs_min.sli).

Please cite this article as: Huntington, J., et al., Assessing the role of climate and resource management on groundwater dependent ecosystem changes in arid environments with the Lan..., Remote Sensing of Environment (2016), http://dx.doi.org/10.1016/j.rse.2016.07.004

classes of the LANDFIRE vegetation map (USGS, 2010) to determine how OLI must be rescaled to match ETM+, and to examine the degree to which differences might be dependent on vegetation class type. Vegetation-dependent changes in NDVI are detected if different classes exhibit differing spectral reflectance distributions within the narrower OLI bands as compared to the broader ETM+ bands.

Two methods of radiometric and atmospheric corrections were tested with the Landsat imagery, 1) the Landsat surface reflectance climate data record provided through the ESPA on-demand interface of the USGS EROS Data Center (Masek et al., 2006; USGS, 2015a), and 2) a method following Tasumi et al. (2008) and Trezza and Allen (2013). The ESPA surface reflectance product uses the USGS Landsat Ecosystem Disturbance Adaptive Processing System (LEDAPS) software for Thematic Mapper imagery from Landsats 5 and 7, and the preliminary USGS L8SR (Landsat 8 Surface Reflectance) software for OLI imagery (USGS, 2015a). The Tasumi/Trezza method was implemented within EE with spatially distributed, near-surface hourly vapor pressure from the North American Land Data Assimilation System (NLDAS; Mitchell et al., 2004) to estimate precipitable water and atmospheric transmittance (Tasumi et al., 2008). Spatially distributed atmospheric pressure was estimated from the 30 m National Elevation Dataset (NED) following ASCE-EWRI (2005).

While the under-flight of Landsat 8 was nearly contemporaneous with Landsat 7, the two paths were not identical (Fig. 1) - the ETM+ scan line corrector mirror created data gaps, and clouds moved between acquisitions. As such, a mask of the most consistent regions between the two sensors was required for inter-sensor calibration. Clouds and cloud shadows in both images were manually masked out with a buffer distance of approximately 1 km to ensure that gradients and cloud cover and haze were removed. Areas with a NIR reflectance of <0.05 were masked out to remove water bodies and areas of deep shadow that affect NDVI. Pixels on either side of boundaries between classes in the LANDFIRE map were removed to reduce the influence of map misregistration, as well as misregistration between the two satellite overpasses in areas of high relief that arose from the offset in overpass position. LANDFIRE classes with masked areas containing <1000 pixels were removed from the analysis to ensure that a stable mean value was calculated for each land cover class. The mean red, NIR, and NDVI for each vegetation class was calculated, and OLI mean values were regressed against ETM+ to determine the appropriate transformation to make NDVI from OLI consistent with the prior sensors.

4.2. Data preparation for GDE assessments

Boundaries were defined around the six study areas (Figs. 2–4) and used to spatially and temporally average summer NDVI derived from cloud-free Landsat images that were closest in time to the middle of June, July, and August from 1985 to 2014. For riparian restoration study sites, average summer NDVI was computed from July–August Landsat images so that the potential for standing water to decrease NDVI was minimized. Based on results of the sensor cross-calibration (detailed in the Results section), NDVI was computed using the Tasumi/Trezza at-surface reflectance method. NDVI was chosen over other indices (i.e. Soil Adjusted Vegetation Index or Modified Soil Adjusted Vegetation Index) since NDVI has the breadth and history of usage that is not matched by other indices, is a popular standard measure, does not require soil parameter calibration, and has been shown to outperform other indices for quantifying sparse vegetation cover in arid environments (McGwire et al., 1999; Wu, 2014). To detect the signal of interannual groundwater availability within GDEs, it was important to focus on periods when shallow soils were dry, and when spectral variability due to the happenstance timing of individual precipitation events was minimized. Precipitation over the study areas is generally at its minimum in June for the more southern and eastern study areas, and in July and August for the northern study areas. Images acquired during the summer months of June–August were selected to limit the NDVI signal of shallow rooted grasses and forbs, and maximize the phreatophyte NDVI signal derived from groundwater.

Summer streamflow, spring flow, and shallow groundwater levels in the Great Basin are highly correlated to annual precipitation due to the fact that the majority of annual precipitation falls during winter as snow, and spring snowmelt provides the majority of groundwater recharge that is later discharged during summer and fall (Huntington and Niswonger, 2012; McEvoy et al., 2012). Water-year (October–September) precipitation (PPT) for each study site was estimated from a hybrid 4 km spatial resolution gridded weather dataset, GRIDMET (Abatzoglou, 2013), based on the Parameter Regression on Independent Slopes Model (PRISM) (Daly et al., 1994) and NLDAS (Mitchell et al., 2004). Evaporative demand (ET_0) was estimated using the standardized Penman-Monteith equation, which is a function of daily solar radiation, air temperature, humidity, and wind speed (ASCE-EWRI, 2005). Daily GRIDMET data were accessed within EE to estimate water-year PPT and ET_0 totals at each study site.

Groundwater level data from the Arlemont Ranch well located within the Fish Lake Valley study area (Fig. 4a), was acquired from the Nevada Division of Water Resources water level database (NDWR, 2015). Two water level readings per year were typically reported, therefore an average of the two readings was computed for each year. Groundwater level and nearby agricultural pumping data for the Needle Point Spring study area (Fig. 4b) was acquired from Summers (2001) and Halford (2015). Annual average groundwater levels and pumping rates were compared with summer NDVI and water-year PPT and ET_0 to assess historical vegetation response to climate and changing groundwater levels.

5. Results

5.1. Sensor cross-calibration

Average LANDFIRE vegetation class red, NIR, and NDVI values derived from USGS ESPA products and the Tasumi/Trezza method are illustrated in Fig. 6. The Tasumi/Trezza method shows a markedly higher degree of correspondence in NDVI between ETM+ and OLI observations. The greater degree of scatter observed in the ESPA plots is likely due to the mixing of atmospheric correction methods between sensors, and limitations the current L8SR software has for areas of high topography (USGS, 2015a). Due to the close correspondence in NDVI between ETM+ and OLI observations, results presented in the following sections were derived solely from the Tasumi/Trezza method.

As might be expected by the greater difference in bandwidths, scatter in Fig. 6 is more pronounced in the NIR than in the red band. While regression residuals for NDVI were relatively small (maximum absolute value <0.02), the four most under-predicted classes in Fig. 6 were all mixed conifer classes, while the two most over-predicted classes contained Gambel oak *(Quercus gambelii)*. This suggests that some vegetation communities did have a detectable difference in spectral reflectance between the ETM+ and OLI bandwidths. However, there were seven other conifer classes that were quite close to the regression line, so a generalization about conifers could not be made. None of the vegetation classes that appear as outliers (Fig. 6) are present in the study areas. The Tasumi/Trezza NDVI regression in Fig. 6 was applied in the EE workflow to compute OLI NDVI for each of the six study areas.

5.2. Baseline assessment of vegetation and climate

Interannual variations of vegetation vigor and climate for Spring Valley and Indian Valley study areas are illustrated by plotting summer NDVI with annual PPT and ET_0 (Figs. 7 and 8). Results show that NDVI and PPT time series co-vary and have similar long-term trends (Fig. 7). While it is evident that NDVI co-varies with annual PPT, statistical correlation between the two variables is only moderate, with R^2 values of 0.49 and 0.41 for Spring Valley and Indian Valley, respectively.

Please cite this article as: Huntington, J., et al., Assessing the role of climate and resource management on groundwater dependent ecosystem changes in arid environments with the Lan..., Remote Sensing of Environment (2016), http://dx.doi.org/10.1016/j.rse.2016.07.004

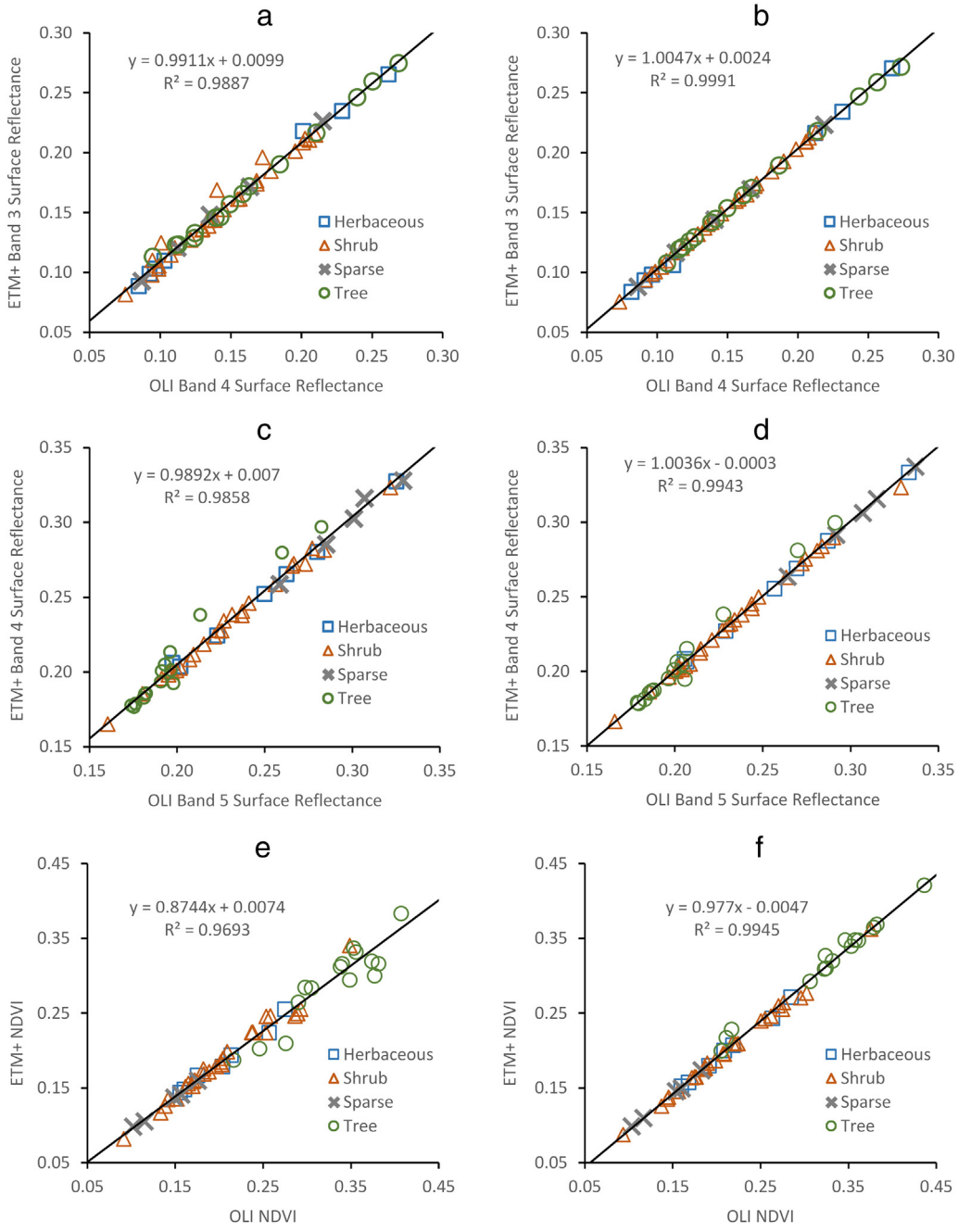

Fig. 6. Mean values of ETM + versus OLI in LANDFIRE vegetation classes for red (a, b), NIR (c, d), and NDVI (e, f) using USGS ESPA Landsat surface reflectance products (a, c, e) and Tasumi/Trezza at-surface reflectance (b, d, f). Symbols indicate the generalized life form attribute of each vegetation class.

Factors limiting the strength of the relationship between annual PPT and summer average NDVI could include: 1) antecedent soil moisture conditions, 2) sparse leaf area of Spring Valley setting a lower limit on detectability; 3) influence of background soil reflectance; 4) presence of shallow groundwater stabilizing minimum vegetation vigor and NDVI, and 5) wide range in NDVI during summer months as illustrated by maximum and minimum values shown in Fig. 7. The deeply rooted phreatophytes of Spring Valley appear to be buffered against years with extremely low PPT more than the shallow rooted meadow grass in Indian Valley (i.e. multi-year drought periods of 1989 to 1994).

Annual vegetation and near-surface atmospheric and climatic feedbacks are evaluated by plotting summer average NDVI and annual ET_0 on the y-axes, with annual PPT on the x-axis (Fig. 8). Illustrating PPT and ET_0 with vegetation and land surface states and fluxes is useful for evaluating the well-known complementary relationship between actual ET and ET_0 in arid environments (Brutsaert and Stricker, 1979; Hobbins et al., 2004; Huntington et al., 2011; Jaksa et al., 2013). The use of summer vegetation indices as proxies for phreatophyte annual ET has been well established within the Great Basin (Nichols, 2000; Groeneveld et al., 2007; Smith et al., 2007; Beamer et al., 2013; Garcia et al., 2014). Fig. 8 illustrates that as annual PPT increases, NDVI increases and ET_0 decreases. Conversely, as PPT decreases, so does NDVI, while ET_0 increases.

These results are consistent with land surface energy balance theory. When water is limited, and available energy is fairly uniform in space, energy that would have been used for ET is instead used in the production of sensible heat flux, thereby increasing air temperature, vapor pressure deficit, and ultimately ET_0 (Brutsaert and Stricker, 1979). This drying scenario is well illustrated in Fig. 8, where ET_0 increases as PPT and NDVI decrease. The complementary relationship between actual ET and ET_0 has been shown to be prevalent at multiple time scales in

Please cite this article as: Huntington, J., et al., Assessing the role of climate and resource management on groundwater dependent ecosystem changes in arid environments with the Lan..., Remote Sensing of Environment (2016), http://dx.doi.org/10.1016/j.rse.2016.07.004

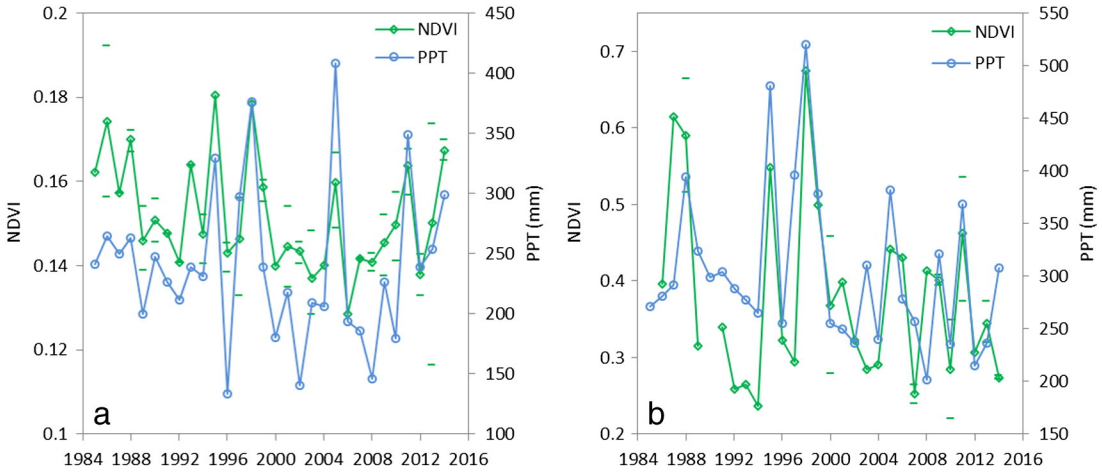

Fig. 7. Spatially averaged summer NDVI and annual PPT time series for Spring Valley (a) and Indian Valley (b) phreatophyte shrub and meadow vegetation study areas. NDVI tics represent June–August maximum and minimum NDVI values. Years with missing maximum and minimum NDVI tics indicate that only one image was available.

Spring Valley and other phreatophyte shrub areas in Nevada using measured energy balance data (Huntington et al., 2011; Beamer et al., 2013). These results clearly highlight the complementary relationship between vegetation vigor, ET_0, and PPT, and are consistent with similar remotely sensed vegetation index and complementary relationship studies (Goward et al., 1994; Szilagyi, 2002; Mo et al., 2014). The long time history of Landsat allows for baseline variability of vegetation vigor and complementary relationships between vegetation and climate to be established at local to regional scales.

5.3. Riparian restoration

The ecological benefits from watershed restoration of Maggie Creek and Susie Creek have been previously well documented (Elliott et al., 2004; Williams et al., 2015). However, interannual Landsat time series of vegetation vigor offer a new perspective for evaluating how riparian areas within these restored watersheds have responded to multiple drought cycles over several decades. Watershed and riparian area restoration efforts within the Maggie and Susie Creek drainages began in the early 1990s, and since that time riparian area NDVI has markedly increased (Fig. 9). Maggie and Susie Creek NDVI trends from 1985 to 2014 are statistically significant at the 95% confidence level using the Mann-Kendall trend test (Helsel and Hirsch, 1992), with *p*-values of 1.4E−06 and 4.1E−04, respectively. July–August maximum and minimum NDVI trends are also statistically significant for both sites (*p*-values of 1.8E−04 and 4.1E−05 for Maggie Creek, and 1.7E−03 and 3.1E−03 for Susie Creek, respectively). A more direct metric of vegetation change since restoration is the percent increase in July–August average NDVI from pre- to post-restoration periods (1985–1989 and 1990–2014). Maggie Creek NDVI increased by 54% from 0.288 to 0.444, and Susie Creek NDVI increased by 67% from 0.236 to 0.396. Average annual PPT increase from pre- to post-restoration was 13% and 14% for Maggie and Susie Creek, respectively, so only part of the post-restoration NDVI increase can be attributed to increased PPT and streamflow given that annual PPT and annual and summer streamflow are highly correlated in this region (Berger, 2000; Prudic et al., 2006; McEvoy et al., 2012). An important attribute of successful riparian restoration is reduced drought stress (Stromberg, 2001; Shafroth et al., 2002). Reduced drought stress since restoration is evident during droughts of the late 1990s and early 2000s, 2007 and 2008, and 2012 and 2013, by the increase of July–August average, maximum, and minimum NDVI values illustrated in Fig. 9.

5.4. Groundwater level changes

Annual PPT, groundwater level, and corresponding summer NDVI changes for the Fish Lake study area are illustrated in Fig. 10. Groundwater levels have steadily decreased since 1979 due to groundwater

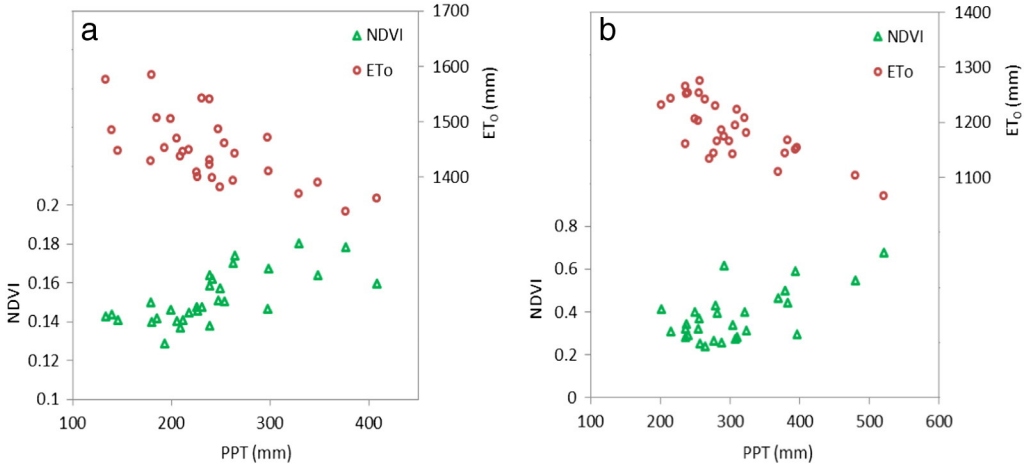

Fig. 8. Spring Valley (a) and Indian Valley (b) summer NDVI, annual ET_0, and PPT, showing a complementary relationship between NDVI and ET_0. As NDVI (i.e. proxy for ET) generally increases with PPT, ET_0 decreases due to near surface atmospheric feedbacks.

Please cite this article as: Huntington, J., et al., Assessing the role of climate and resource management on groundwater dependent ecosystem changes in arid environments with the Lan..., Remote Sensing of Environment (2016), http://dx.doi.org/10.1016/j.rse.2016.07.004

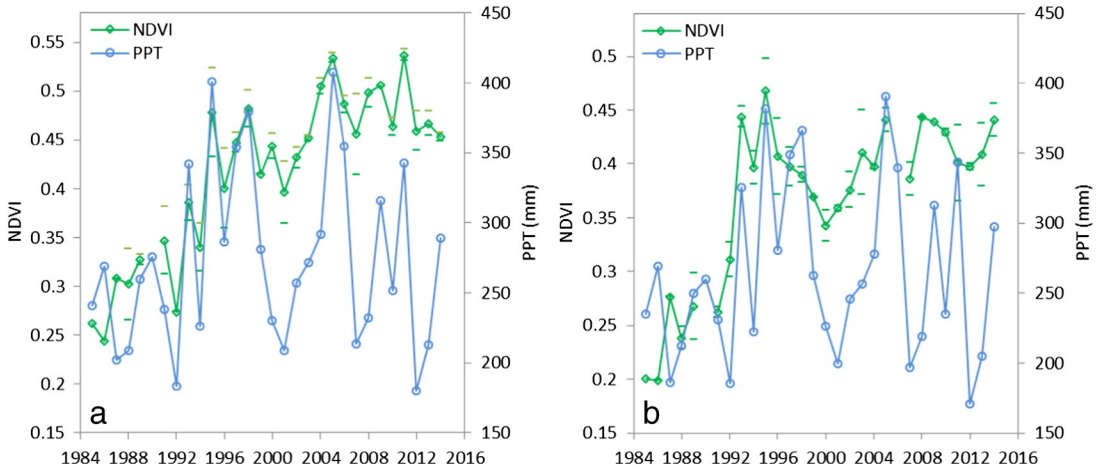

Fig. 9. Spatially averaged July–August NDVI and annual PPT time series for Maggie Creek (a) and Susie Creek (b) riparian restoration sites. NDVI tics represent July–August maximum and minimum NDVI values.

pumping for irrigated agriculture adjacent to the study area (Fig. 4). Depth to groundwater was approximately 5 m in 1985, and has declined at a rate of ~0.167 m/year to reach a depth of 10 m in 2014. NDVI has also declined during the period of groundwater level decline, with intermittent NDVI increases that correspond to anomalously high annual PPT. The trend of June–August average NDVI from 1985 to 2014 is statistically significant at the 95% confidence level, with a *p*-value of 4.2E−06. Summer maximum and minimum NDVI trends from 1985 to 2014 are also statistically significant, with *p*-values of 6.9E−04 and 8.7E−05, respectively.

Figs. 11 and 12 illustrate spatially averaged summer NDVI paired with annual PPT, depth to groundwater, groundwater pumping, and ET_0 for the Needle Point Spring study area, where it is observed that NDVI begins to decline following the year 1999, and is coincident with the onset of pumping and drought. According to Summers (2001), Needle Point spring ceased flowing in 2001. NDVI has continued to decline since 2001, with NDVI increases that coincide with years of anomalously high annual PPT. The downward trend in NDVI from 1985 to 2014 is statistically significant at the 95% confidence level (*p*-value of 3.4E−04), and there is a slight positive trend in PPT during this same period. Summer maximum and minimum NDVI trends are also statistically significant, with *p*-values of 3.7E−03 for both maximum and minimum NDVI. Average summer NDVI for pre- and post-groundwater pumping periods (1986–1999 and 2000–2014) was 0.37 and 0.29, respectively, which equates to a 22% decrease. Average annual PPT was 239 and 221 mm for pre- and post-groundwater pumping periods, an 8% decrease. These results suggest that the post-pumping NDVI decline (2000 to 2014) could be partly attributed to lower annual PPT. However, given the supporting evidence of measured and simulated groundwater level declines (Summers, 2001; Halford, 2015), long-term NDVI declines are most likely related to groundwater pumping adjacent to the spring area (Fig. 12a). Reduced maximum, minimum, and average summer NDVI peaks during post-pumping further support this hypothesis. For example, average NDVI values coincident with anomalously high PPT years of 2005 and 2011 never reach the pre-pumping average NDVI of 0.37 (Fig. 11b). Additionally, the relationship between PPT and NDVI markedly changed during the post-pumping period (Fig. 12b).

6. Discussion

Isolating the impacts of natural climatic and hydrologic variability on vegetation vigor, from of the impacts of anthropogenic land and water management is challenging, yet important for identifying cause and effect relationships. Having the ability to readily evaluate lengthy and paired time series of climate and Landsat derived vegetation vigor, offers land and water managers new and valuable information for long-term assessment of GDEs. Such lengthy Landsat derived time series require effective sensor cross-calibration so that cause and effect are not misinterpreted (Roy et al., 2016). Fig. 6 demonstrates the importance of using a consistent atmospheric correction method across sensor systems. The magnitude of OLI/ETM+ NDVI regression residuals using the ESPA products was double that of the Tasumi/Trezza method.

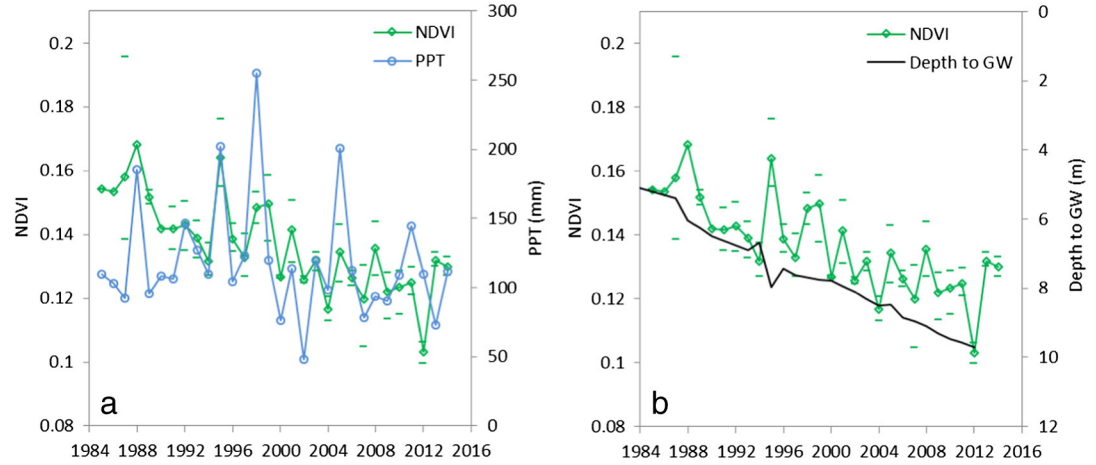

Fig. 10. Spatially averaged summer NDVI and annual PPT time series (a) and spatially averaged summer NDVI and average depth to groundwater (b) for the Fish Lake Valley study area. NDVI time series illustrate a general decline as depth to groundwater increases. NDVI tics represent June–August maximum and minimum NDVI values.

Please cite this article as: Huntington, J., et al., Assessing the role of climate and resource management on groundwater dependent ecosystem changes in arid environments with the Lan..., Remote Sensing of Environment (2016), http://dx.doi.org/10.1016/j.rse.2016.07.004

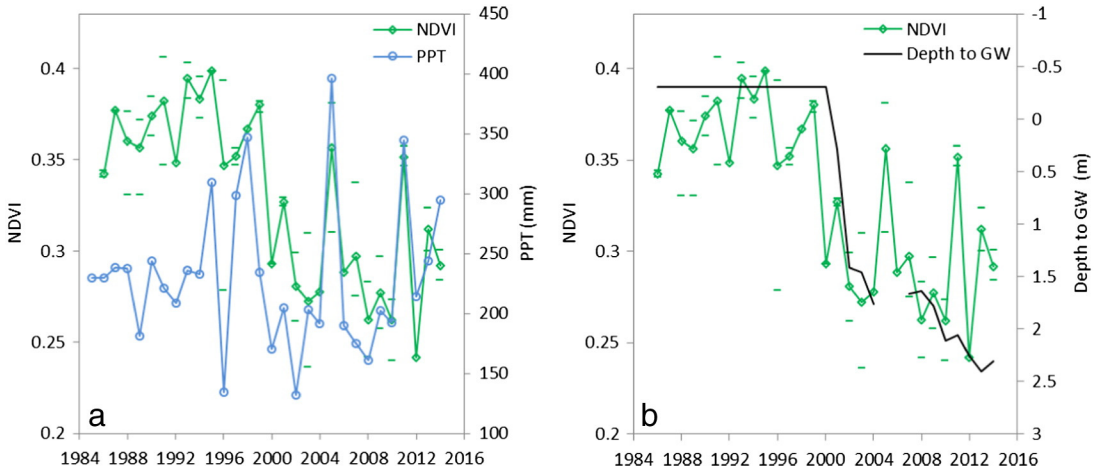

Fig. 11. Spatially averaged summer NDVI and annual PPT time series (a) and spatially averaged summer NDVI and average depth to groundwater (b) for the Needle Point Spring study area. NDVI tics represent June–August maximum and minimum NDVI values.

While the use of differing atmospheric correction algorithms from ESPA may be dictated by operational data processing flows, consistent implementation of the Tasumi/Trezza method using EE cloud computing allowed rapid on-demand processing and delivery to the desktop computer with consistent image data products. The near-contemporaneous collection of images during the Landsat 8 under-fly testing period, and our averaging of NDVI within boundary-masked areas of different vegetation classes, essentially eliminated the effects spatiotemporal misregistration on the regressions of Fig. 6. The high level of correspondence between Tasumi/Trezza-corrected NDVI across a wide variety of natural vegetation communities suggests that the dramatic change in NIR bandwidths from ETM + to OLI is well corrected by linear regression and should not generally interfere with time series analyses. These findings suggest that vegetation index analyses originating from different Landsat sensors can be made easily compatible, allowing seamless analysis over the entire archive. However, the consistency of species composition among the most positive and the most negative regression residuals indicates that land-cover specific adjustments may be, in some cases, necessary.

While time series analyses of Landsat data over spatially limited study areas are often powerful and enlightening, cloud storage computing capabilities (i.e., co-located storage and parallel processing of Landsat, meteorology, and climate datasets with geospatial analysis capabilities) provided by EE make it possible to easily and rapidly spatially up-scale. A computation that would take a single computer minutes to hours can be performed in a matter of seconds. This allows for exploration of multiple interannual temporal and spatial signals over large regions. Large scale spatiotemporal analyses, previously precluded due to massive storage and computational volumes, are for the first time, practical due to geospatially-enabled cloud computing systems. However, regardless of newly available computing power, a limitation with respect to seasonal and interannual time series analysis is the limited number of cloud free Landsat images available for time periods of interest (e.g. 8 or 16 day returns for calculation of one to three month summer maximum, minimum, and average NDVI). Integration of newly available Sentinel 2 imagery with Landsat processing workflow will increase the probability of cloud free images available for seasonal and interannual time series analysis.

Future research that combines both time series and spatial analyses will greatly enhance our ability to rapidly evaluate the magnitude, spatial extent, and cause of GDE changes related to climate, land, and water management (Kennedy et al., 2014). Sophisticated tools for Landsat spatial time series analysis that have traditionally been focused on forest disturbance and recovery such as LandTrendr and TimeSync (Kennedy et al., 2010; Cohen et al., 2010), could prove extremely useful for rapid GDE monitoring within EE. Currently, simple products such as Landsat scale NDVI anomalies (i.e. per pixel difference from long-term average) can be rapidly generated within EE to explore and discover relative change, and be combined with climate, meteorological, and field data. For example, Fig. 13 illustrates the Needle Point Spring June–August

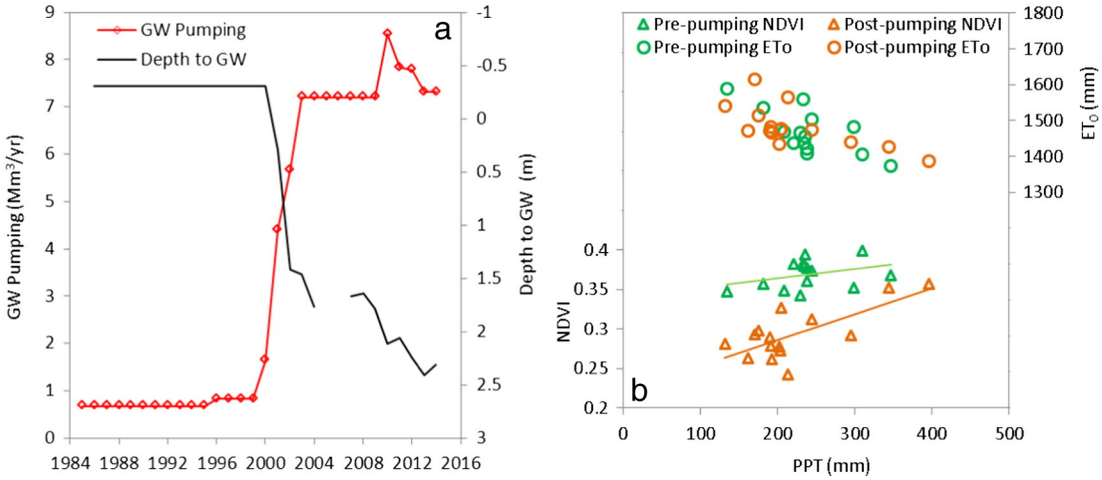

Fig. 12. Groundwater pumping and depth to groundwater for the Needle Point Spring study area (a), and annual PPT, ET_0, and summer NDVI, for pre and post-pumping periods (b).

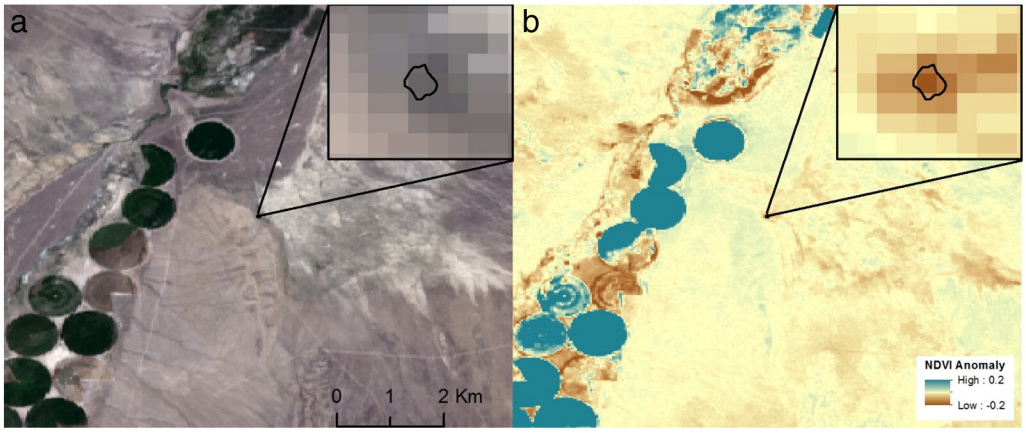

Fig. 13. Needle Point Spring Landsat 8 median true color composite (a), and NDVI anomaly (b), for June–August 2014.

2014 NDVI anomaly (i.e. difference) relative to the 1985 to 2014 average using Landsat 5, 7, and 8 top-of-atmosphere reflectance image collections within EE. While Fig. 13 clearly illustrates that Needle Point Spring has anomalously low NDVI during summer of 2014, it also shows anomalously low NDVI within groundwater discharge areas to the east and southeast of Needle Point Spring (i.e. high reflectance saline soil areas shown in true color image). Conversely, anomalously high NDVI areas primarily occur in non-phreatophyte upland areas to the southwest of Needle Point Spring because of anomalously high rains that occurred during the summer of 2014. Future efforts for regional long-term and interannual GDE monitoring could combine spatial and temporal distributions of vegetation indices with vegetation type, and climatic, meteorologic, and hydrologic distributions to better isolate and analyze natural and anthropogenic impacts.

7. Conclusions

This paper highlights the use of the Landsat archive for monitoring groundwater dependent ecosystems (GDEs). These ecosystems provide critical habitat for many sensitive species in arid and semi-arid environments of phreatophyte shrub lands, meadows, spring areas, and riparian zones. The Landsat archive shows meaningful correlations between changes in annual vegetation vigor (NDVI), precipitation, evaporative demand, depth to groundwater, and land and water management within six GDE study areas. The study approach relied on sensor cross-calibration, cloud computing of Landsat and meteorological data, and statistical evaluation. This approach can provide rapid, useful interpretations of GDE conditions. Results indicate a benefit from the application of a consistent atmospheric correction method across different Landsat sensors. Special attention should be given to whether the observed level of inconsistency in at-surface reflectance for Landsat can be minimized in future operational products. Having demonstrated the ability of the current Landsat archive to detect trends in GDEs related to climate, groundwater, and resource management, that will ultimately fill critical information needs for science-informed decisions, it is clear that a compatible remote sensing data stream must be maintained into the future, and that the value of this consistent growing archive will compound over time. The longevity and continuity of measurements from sensors in the lineage of Landsats provide important baseline and current conditions for ecosystem assessments that would not otherwise be attainable.

Acknowledgments

Funding for this study was provided by the U.S. Bureau of Land Management grant #L13AC00169, U.S. Department of Agriculture Agricultural Research Service grant #59-5370-3-001, Desert Research Institute Maki Endowment, U.S. Geological Survey 2012–2017 Landsat Science Team, Department of the Interior Northwest Climate Science Center grant to evaluate new strategies for addressing climate change impacts on water and ecosystems in the Great Basin, and a Google Earth Engine faculty research grant. ESPA Landsat Surface Reflectance products used were courtesy of the U.S. Geological Survey. The authors would like to thank Stephen Maples of the U.S. Geological Survey, and four anonymous reviewers for their thoughtful comments and suggestions. They greatly improved the manuscript.

References

Abatzoglou, J.T., 2013. Development of gridded surface meteorological data for ecological applications and modelling. International Journal of Climatology 33 (1), 121–131.
Aldridge, C.L., Boyce, M.S., 2007. Linking occurrence and fitness to persistence: Habitat-based approach for endangered greater sage-grouse. Ecological Applications 17 (2), 508–526.
ASCE-EWRI. (2005). The ASCE standardized reference evapotranspiration equation, report 0-7844-0805-X, ASCE task committee on standardization of reference evapotranspiration, Reston, Virginia, American Society of Civil Engineers. (Available at) http://www. kimberly.uidaho.edu/water/asceewri/
Beamer, J.P., Huntington, J.L., Morton, C.G., Pohll, G.M., 2013. Estimating annual groundwater evapotranspiration from phreatophytes in the great basin using landsat and flux tower measurements. JAWRA Journal of the American Water Resources Association 49 (3), 518–533.
Berger, D.L., 2000. Water budgets for pine valley, Carico lake valley, and upper Reese river valley hydrographic areas, middle Humboldt river basin, north-central Nevada methods for estimation and results: U.S. geological survey water-resources investigation report 99-4272 (45 p).
BLM (Bureau of Land Management). 2012. White paper on BLM and U.S. forest service greater Sage-Grouse preliminary habitat map. Available at http://www.blm.gov/nv/st/en/prog/wildlife/greater_sage-grouse/preliminary_habitat.html
Bredehoeft, J.D., 2002. The water budget myth revisited: Why hydrogeologists model. Groundwater 40 (4), 340–345.
Bredehoeft, J.D., Papadopulos, S.S., Cooper, H.J., 1982. Groundwater: The water budget myth. Scientific basis of water resource management, National Academy of Sciences Studies in Geophysics. pp. 51–57.
Brutsaert, W., Stricker, H., 1979. An advection-aridity approach to estimate actual regional evapotranspiration. Water Resources Research 15 (2), 443–450.
Burns, A.G., Drici, W., 2011. June. Hydrology and water resources of spring, cave, dry lake, and Delamar valleys, Nevada and vicinity. Presentation to the Office of the Nevada State Engineer: Southern Nevada Water Authority, Las Vegas, Nevada.
BWG (Biological Work Group), 2009. Biological monitoring plan for the spring valley stipulation. (February 2009). (Available at) http://www.fws.gov/nevada/highlights/comment/spring_valley/Biological_Monitoring_Plan_Spring_Valley_Stipulation_Feb_09.pdf.
Childress, J.M., Smith, D.L., 2015. Exhibit 54, public administrative hearing before the state engineer in the matter of protested applications 78795, etc., February 2–6, 2015, official records in the Office of the State Engineer.
Chimner, R.A., Cooper, D.J., 2004. Using stable oxygen isotopes to quantify the water source used for transpiration by native shrubs in the San Luis Valley, Colorado USA. Plant and Soil 260 (1–2), 225–236.
Clark, R.N., Swayze, G.A., Wise, R., Livo, K.E., Hoefen, T.M., Kokaly, R.F., Sutley, S.J., 2007. USGS digital spectral library splib06a, U.S. geological survey, data series 231..
Cohen, W.B., Yang, Z., Kennedy, R., 2010. Detecting trends in forest disturbance and recovery using yearly landsat time series: 2. TimeSync—Tools for calibration and validation. Remote Sensing of Environment 114 (12), 2911–2924.
Cooper, D.J., Sanderson, J.S., Stannard, D.I., Groeneveld, D.P., 2006. Effects of long-term water table drawdown on evapotranspiration and vegetation in an arid region phreatophyte community. Journal of Hydrology 325 (1), 21–34.

Daly, C., Neilson, R.P., Phillips, D.L., 1994. A statistical-topographic model for mapping climatological precipitation over mountainous terrain. Journal of Applied Meteorology 33 (2), 140–158.

Dawson, T.E., Pate, J.S., 1996. Seasonal water uptake and movement in root systems of Australian phreatophytic plants of dimorphic root morphology—A stable isotope investigation. Oecologia 107, 13–20.

DOI (Department of the Interior), 2015. Endangered and threatened wildlife and plants; 12-month finding on a petition to list greater Sage-Grouse (*Centrocercus urophasianus*) as an endangered or threatened species; proposed rule. Fish and wildlife service, 50 CFR Part 17. Federal register Vol. 80. No. 191.

Donnelly, J.P., Naugle, D.E., Hagen, C.A., Maestas, J.D., 2016. Public lands and private waters: Scarce mesic resources structure land tenure and sage-grouse distributions. Ecosphere 7 (1).

Elliott, J., Haskins, R.L., Weller, G., 2004. Lahontan cutthroat trout species management plan for the upper Humboldt river drainage basin. State of Nevada, Department of Wildlife.

Elmore, A.J., Mustard, J.F., Manning, S.J., 2003. Regional patterns of plant community response to changes in water: Owens Valley, California. Ecological Applications 13 (2).

Elmore, A.J., Manning, S.J., Mustard, J.F., Craine, J.M., 2006. Decline in alkali meadow vegetation cover in California: The effects of groundwater extraction and drought. Journal of Applied Ecology 43 (4), 770–779.

Garcia, C.A., Huntington, J.M., Buto, S.G., Moreo, M.T., Smith, J.L., Andraski, B.J., 2014. Groundwater discharge by evapotranspiration, Dixie Valley, west-central Nevada, March 2009–September 2011 (No. 1805). US geological survey.

Glancy, P.A., Rush, F.E., 1968. Water-resources appraisal of smoke creek-San Emidio desert area, Nevada and California: Nevada Department of Conservation and Natural Resources, Water Resources–Reconnaissance series report. 44 (57 p).

Goward, S.N., Waring, R.H., Dye, D.G., Yang, J., 1994. Ecological remote sensing at OTTER: Satellite macroscale observations. Ecological Applications 322–343.

Groeneveld, D.P., 2008. Remotely-sensed groundwater evapotranspiration from alkali scrub affected by declining water table. Journal of Hydrology 358 (3), 294–303.

Groeneveld, D.P., Baugh, W.M., Sanderson, J.S., Cooper, D.J., 2007. Annual groundwater evapotranspiration mapped from single satellite scenes. Journal of Hydrology 344 (1), 146–156.

Halford, K.J., 2015. Exhibit 153, public administrative hearing before the state engineer in the matter of protested applications 78795, etc., February 2–6, 2015, official records in the Office of the State Engineer.

Helsel, D.R., Hirsch, R.M., 1992. Statistical methods in water resources. 49. Elsevier.

Hobbins, M.T., Ramírez, J.A., Brown, T.C., 2004. Trends in pan evaporation and actual evapotranspiration across the conterminous US: Paradoxical or complementary? Geophysical Research Letters 31 (13).

Homer, C.G., Xian, G., Aldridge, C.L., Meyer, D.K., Loveland, T.R., O'Donnell, M.S., 2015. Forecasting sagebrush ecosystem components and greater sage-grouse habitat for 2050: Learning from past climate patterns and landsat imagery to predict the future. Ecological Indicators 55, 131–145.

Huntington, J.L., Niswonger, R.G., 2012. Role of surface-water and groundwater interactions on projected summertime streamflow in snow dominated regions: An integrated modeling approach. Water Resources Research 48 (11).

Huntington, J.L., Szilagyi, J., Tyler, S.W., Pohll, G.M., 2011. Evaluating the complementary relationship for estimating evapotranspiration from arid shrublands. Water Resources Research 47 (5).

Irish, R.R., Barker, J.L., Goward, S.N., Arvidson, T., 2006. Characterization of the landsat-7 ETM+ automated cloud-cover assessment (ACCA) algorithm. Photogrammetric Engineering and Remote Sensing 72 (10), 1179–1188.

Jaksa, W.T., Sridhar, V., Huntington, J.L., Khanal, M., 2013. Evaluation of the complementary relationship using Noah land surface model and north American regional reanalysis (NARR) data to estimate evapotranspiration in semiarid ecosystems. Journal of Hydrometeorology 14 (1), 345–359.

Kennedy, R.E., Yang, Z., Cohen, W.B., 2010. Detecting trends in forest disturbance and recovery using yearly landsat time series: 1. LandTrendr—Temporal segmentation algorithms. Remote Sensing of Environment 114 (12), 2897–2910.

Kennedy, R.E., Andréfouët, S., Cohen, W.B., Gómez, C., Griffiths, P., Hais, M., ... Zhu, Z., 2014. Bringing an ecological view of change to landsat-based remote sensing. Frontiers in Ecology and the Environment 12 (6), 339–346.

Li, P., Jiang, L., Feng, Z., 2013. Cross-comparison of vegetation indices derived from landsat-7 enhanced thematic mapper plus (ETM+) and landsat-8 operational land imager (OLI) sensors. Remote Sensing 6 (1), 310–329.

Martínez-Beltrán, C., Jochum, M.O., Calera, A., Melia, J., 2009. Multisensor comparison of NDVI for a semi-arid environment in Spain. International Journal of Remote Sensing 30 (5), 1355–1384.

Masek, J.G., Vermote, E.F., Saleous, N.E., Wolfe, R., Hall, F.G., Huemmrich, K.F., ... Lim, T.K., 2006. A landsat surface reflectance dataset for North America, 1990–2000. Geoscience and Remote Sensing Letters IEEE 3 (1), 68–72.

McEvoy, D.J., Huntington, J.L., Abatzoglou, J.T., Edwards, L.M., 2012. An evaluation of multiscalar drought indices in Nevada and Eastern California. Earth Interactions 16 (18), 1–18.

McGwire, K., Minor, T., Fenstermaker, L., 1999. Hyperspectral mixture modeling for quantifying sparse vegetation cover in arid environments. Remote Sensing of Environment 72, 360–374.

Mitchell, K.E., Lohmann, D., Houser, P.R., Wood, E.F., Schaake, J.C., Robock, A., ... Bailey, A.A., 2004. The multi-institution North American Land Data Assimilation System (NLDAS): Utilizing multiple GCIP products and partners in a continental distributed hydrological modeling system. Journal of Geophysical Research - Atmospheres 109, D7 (1984–2012).

Mo, X., Liu, S., Lin, Z., Wang, S., Hu, S., 2014. Trends in land surface evapotranspiration across China with remotely sensed NDVI and climatological data for 1981–2010. Hydrological Sciences Journal.

Moreo, M.T., Laczniak, R.J., Stannard, D.I., 2007. Evapotranspiration rate measurements of vegetation typical of ground-water discharge areas in the basin and range carbonate-rock aquifer system, white Pine County, Nevada, and adjacent areas in Nevada and Utah, September 2005–August 2006. US geological survey. pp. 443–460.

Naumburg, E., Mata-Gonzalez, R., Hunter, R.G., Mclendon, T., Martin, D.W., 2005. Phreatophytic vegetation and groundwater fluctuations: A review of current research and application of ecosystem response modeling with an emphasis on Great Basin vegetation. Environmental Management 35 (6), 726–740.

NDWR (Nevada Division of Water Resources), 2015. Water level database. accessed on April, 20, 2015 http://water.nv.gov/data/waterlevel/.

Nguyen, U., Glenn, E.P., Nagler, P.L., Scott, R.L., 2014. Long-term decrease in satellite vegetation indices in response to environmental variables in an iconic desert riparian ecosystem: The Upper San Pedro, Arizona, United States. Ecohydrology.

Nichols, W.D., 2000. Regional ground-water evapotranspiration and ground-water budgets. Great Basin, Nevada (No. 1628).

NSEO (The Office of the State Engineer of the State of Nevada), 2012a. The ruling (#6164) in the matter of applications 54003 through 54021, inclusive, filed to appropriate the underground waters of the spring valley hydrographic basin (184). Nevada: Lincoln and White Pine Counties (218 pp.).

Patten, D.T., Rouse, L., Stromberg, J.C., 2008. Isolated spring wetlands in the Great Basin and Mojave deserts, USA: Potential response of vegetation to groundwater withdrawal. Environmental Management 41 (3), 398–413.

Pritchett, D., Manning, S.J., 2012. Response of an intermountain groundwater-dependent ecosystem to water table drawdown. Western North American Naturalist 72 (1), 48–59.

Prudic, D.E., Niswonger, R.G., Plume, R.W., 2006. Trends in streamflow on the Humboldt River between Elko and Imlay, Nevada, 1950–99. U.S. geological survey scientific investigation report 2005–5199 (58p).

Robinson, T.W. (1958). Phreatophytes: U.S. geological survey water supply paper 1423, 84 p., http://pubs.er.usgs.gov/publication/wsp1423

Roy, D.P., Wulder, M.A., Loveland, T.R., Woodcock, C.E., Allen, R.G., Anderson, M.C., ... Zhu, Z., 2014. Landsat-8: Science and product vision for terrestrial global change research. Remote Sensing of Environment 145, 154–172.

Roy, D.P., Kovalskyy, V., Zhang, H.K., Vermote, E.F., Yan, L., Kumar, S.S., Egorov, A., 2016. Characterization of landsat-7 to landsat-8 reflective wavelength and normalized difference vegetation index continuity. Remote Sensing of Environment.

Shafroth, P.B., Stromberg, J.C., Patten, D.T., 2002. Riparian vegetation response to altered disturbance and stress regimes. Ecological Applications 12 (1), 107–123.

Smith, J.L., Laczniak, R.J., Moreo, M.T., Welborn, T.L., 2007. Mapping evapotranspiration units in the basin and range carbonate-rock aquifer system, White Pine County, Nevada, and adjacent areas in Nevada and Utah: US Geological Survey Scientific Investigations Report 2007–5087 20 p., with downloadable video, accessed November 29, 2010. US Geological Survey Nevada Science Center, Carson City, Nevada.

Steven, M.D., Malthus, T.J., Baret, F., Xu, H., Chopping, M.J., 2003. Intercalibration of vegetation indices from different sensor systems. Remote Sensing of Environment 88 (4), 412–422.

Stromberg, J.C., 2001. Restoration of riparian vegetation in the south-western United States: Importance of flow regimes and fluvial dynamism. Journal of Arid Environments 49 (1), 17–34.

Summers, P., 2001. Hydrogeologic analysis of needle point spring Fillmore Field office, Utah. Bureau of Land Management report 19p.

Szilagyi, J., 2002. Vegetation indices to aid areal evapotranspiration estimations. Journal of Hydrologic Engineering 7 (5), 368–372.

Tasumi, M., Allen, R.G., Trezza, R., 2008. At-surface reflectance and albedo from satellite for operational calculation of land surface energy balance. Journal of Hydrologic Engineering 13 (2), 51–63.

Trezza, R., Allen, R.G., 2013. Report on developing albedo weighting coefficients and surface reflectance coefficients for the Landsat 8 operational land imager. Report by the University of Idaho Kimberly Research and Extension Center. Kimberly, Idaho, p. 15 (rev. 2016).

USGS (U.S. Geological Survey), 2010. LANDFIRE: LANDFIRE 1.1.0, existing vegetation type layer, U.S. Department of the Interior, U.S. geological survey. (Available at) http://landfire.cr.usgs.gov/viewer/.

USGS (U.S. Geological Survey). (2015a). Product guide: Provisional landsat 8 surface reflectance product, version 1.3. (Available at:) http://landsat.usgs.gov/documents/provisional_l8sr_product_guide.pdf. Accessed July 15, 2015.

USGS (U.S. Geological Survey). (2015b). LANDSAT 8 (L8) data users handbook – Version 1, U.S. Department of the Interior, U.S. geological survey. (Available at) https://landsat.usgs.gov/documents/Landsat8DataUsersHandbook.pdf. (Accessed January 17, 2016).

Vogelmann, J.E., Helder, D., Morfitt, R., Choate, M.J., Merchant, J.W., Bulley, H., 2001. Effects of landsat 5 thematic mapper and landsat 7 enhanced thematic mapper plus radiometric and geometric calibrations and corrections on landscape characterization. Remote Sensing of Environment 78 (1), 55–70.

Williams, J.E., Neville, H.M., Haak, A.L., Colyer, W.T., Wenger, S.J., Bradshaw, S., 2015. Climate change adaptation and restoration of western trout streams: Opportunities and strategies. Fisheries 40 (7), 304–317.

Wu, W., 2014. The generalized difference vegetation index (GDVI) for dryland characterization. Remote Sensing 6, 1211–1233.

Yang, X., Smith, P.L., Yu, T., Gao, H., 2011. Estimating evapotranspiration from terrestrial groundwater-dependent ecosystems using landsat images. International Journal of Digital Earth 4 (2), 154–170.

Please cite this article as: Huntington, J., et al., Assessing the role of climate and resource management on groundwater dependent ecosystem changes in arid environments with the Lan..., Remote Sensing of Environment (2016), http://dx.doi.org/10.1016/j.rse.2016.07.004